Sustainable Green Synthesis of Leaf Extract-Stabilized Silver Nanoparticles: Catalytic, Antimicrobial Properties and Colorimetric Sensing of Hg^{2+}

Nasheetha Rahman Thythottathil[1,], Suhaila Thattaril[1,2,] and Kavitha Manniledam[1,*,]

[1]Post Graduate and Research Department of Chemistry, Zamorins Guruvayurappan College, (Affiliated to University of Calicut), Kozhikode-673014, India
[2]Department of Chemistry, Government College, Kodanchery-673580, India

*Corresponding author: E-mail: kavitham@zgcollege.ac.in

Green synthesis of silver nanoparticle(Ag NPs) s employing the aqueous extract of three different dried leaves, *Murraya koenigi*, *Ocimum sanctum* and *Mentha spicata* leaves was carried out. Different techniques, including UV-Visible spectroscopy, dynamic light scattering (DLS), scanning electron microscopy (SEM) and transmission electron microscopy (TEM) were employed to characterize green synthesized silver nanoparticles. The AgNPs are found to have effective catalytic properties in the reduction of 4-nitrophenol and in the degradation of methyl orange and methylene blue dyes. Mercuric ion was selectively detected at ppm level with the green silver nanoparticles. Their antibacterial efficacy was evaluated against both Gram-negative *Pseudomonas fluorescens* and Gram-positive *Bacillus megaterium* bacteria. This study also explores the antifungal properties of green synthesized silver nanoparticles with *Candida albicans* and *Candida parapsilosis*.

Keywords: Silver nanoparticles, *Murraya koenigi*, *Ocimum sanctum*, *Mentha spicata*, Sensing properties, Biological activity.

INTRODUCTION

Green synthesis offers a diverse range of economically benign ecofriendly design for the synthesis of metal nanoparticles. The synthesis of metal or metal oxide nanoparticles through the use of plants stands out among other eco-friendly methods as a straightforward and efficient approach for large-scale nanoparticle production. This is a suitable alternative to chemical and physical methods for the synthesis of metal nanoparticles [1]. Furthermore, green synthesis presents an attractive avenue for the sustainable production of silver nanoparticles, with potential benefits spanning multiple industries and research fields [2].

Among the various noble metals, silver is the metal of first choice due to their diverse properties especially high catalytic nature in chemical reactions, antibacterial, antifungal and antioxidant properties [3-5]. The size of biosynthesized Ag NPs strongly influences their catalytic and antimicrobial properties. Smaller Ag NPs show better performance than larger Ag NPs [6-10]. Nano silver acts as an effective germ-killing agent against a broad spectrum of infectious microorganisms which

is effectively adsorbed on it and silver nanoparticles enter into the pathogen and blocking DNA, also they denatured the enzymes which is used for the transportation of nutrients [11,12]. As a result of strong antimicrobial activity silver nanoparticles used in day-to-day life products such as soap, toothpaste, dental materials and composites, stainless steels, in human skin, in water purification system, medical devices cosmetics, bioremediation of heavy metal and pesticide removal in water and soil [13,14], wound dressings, antibacterial coatings for medical devices, antimicrobial agents in healthcare settings, antibacterial sprays, in clothing, bed linens, fabric-based products, used in food packaging materials to extend shelf life by inhibiting microbial growth and preventing food spoilage and used in cosmetics and personal care products for their antimicrobial properties and as UV blockers in sunscreens [15-23].

Nano-catalysts represent a promising approach for mitigating the environmental impact of synthetic dyes in industries like textiles, pharmaceuticals and wastewater treatment. Organic dyes have been traditionally used in various industries for colouring purposes due to their versatility and wide range of hues. However, many synthetic dyes contain toxic chemicals

that can be harmful to both human health and the environment. Moreover, when these synthetic dyes are released into the environment, they can pollute waterways, harm aquatic life and disrupt ecosystems. Additionally, the production process for synthetic dyes often involves the use of non-renewable resources and generates significant amounts of waste and pollution [24-26]. Green synthesized metal nanoparticles have also shown promise as highly efficient catalysts for the reduction or degradation of organic dyes. This affordability and high yield make Ag NPs attractive for various applications, including catalysis for organic transformation reactions [27-30].

The leaf extracts can act as effective reducing agents for metal ions, facilitating the synthesis of metal nanoparticles. Furthermore, their involvement extends to the stabilization of the nanoparticles, mitigating the risk of agglomeration and ensuring the preservation of desired particle properties. In this work, *Murraya koenigi*, *Oscimum sanctum* and *Mentha spicata* leaves extract were utilized for the synthesis of silver nanoparticles with certain biological activities, evaluation of their efficiency in sensing selective heavy metal ions and as photocatalyst in the the degradation of dyes.

EXPERIMENTAL

Fresh leaves of *Murraya koenigii* (curry leaves), *Ocimum sanctum* (Tulasi leaves) and *Mentha spicata* (mint leaves) were collected from the local market of Mankavu, Kozhikode city, Kerala, India. Methylene blue and methyl orange dyes were obtained from Nice Chemicals and Thomas Baker, respectively. Sodium borohydride was sourced from Spectrochem and metal salts including mercuric acetate were purchased from Merck Chemicals, Ltd. as well as Nice Chemicals, India.

Preparation of leaf extract: To prepare the leaf extracts, the leaves were thoroughly washed three times with running water and twice with deionized water to remove any debris. They were then sun-dried for 5 days and crushed into a fine powder. For extraction, 5 g of powdered leaves were placed into a 250 mL beaker containing a glass rod and 100 mL of deionized water. The mixture was boiled for 20 min with occasional stirring and then allowed to cool. After cooling, the mixture was filtered three times and the filtered extract was stored at 4 ºC for further analysis. For dilution, 1 mL of crude extract was mixed with 9 mL of deionized water.

Green synthesis of Ag NPs: The plant extract (1 mL) was added to 4 mL of 1×10^{-3} M AgNO$_3$ solution in a 10 mL vial. The mixture was stirred at room temperature for 6 h under dark conditions. A colour change from light yellow to reddish brown indicating the formation of silver nanoparticles. The solution was then allowed to rest for 1 h. The Ag NPs synthesized from *Murraya koenigii* (MK) leaves extract were abbreviated as MK-Ag NPs, *Ocimum sanctum* (OS) as OS-Ag NPs and *Mentha spicata* (MS) as MS-Ag NPs.

Characterization: UV-Visible spectra were recorded using a Shimadzu 1900 UV-Visible spectrophotometer, operating within the wavelength range of 1000 to 200 nm. The morphology of the nanoparticles was examined using a Gemini SEM Carl Zeiss scanning electron microscope. Transmission electron microscopy (TEM) images were acquired with an FEI Technai

T20 and a JEOL JEM-2000 transmission electron microscope, utilizing a carbon-coated Cu grid. Dynamic light scattering (DLS) measurements were performed using a DLS 90 Plus/ BI-MAS system (Brookhaven Instruments, NY) at 25 ºC, with 1 cm path length. The laser wavelength employed was 659 nm and the scattering angle was set to 90º. The viscosity of the solutions was assumed to be equivalent to that of solvent (water). The crystal structure was analyzed using AERIS research bench top X-ray refractometer and patterns were recorded with Cu $K\alpha$ radiation ($\lambda = 1.54060$ Å).

Colorimetric sensing: The synthesized Ag NPs (MK-Ag NPs, MS-Ag NPs and OS-Ag NPs) were utilized for the colorimetric sensing of metal ions. To 5 mL of each bioreduced MK-Ag NPs, MS-Ag NPs and OS-Ag NPs nanoparticle solution, different metal ion solutions (each at a fixed concentration of 10^{-5} M) were added in volumes of 400 μL, 300 μL and 250 μL, respectively. Upon the addition of Hg^{2+}, the solution immediately became colourless, while no significant colour change was observed for the other metal ions. The entire sensibility was monitored by UV-Visible spectrophotometer.

Catalytic studies: The catalytic degradation of methylene blue, methyl orange and 4-nitrophenol was investigated using green-synthesized silver nanoparticles (Ag NPs) in aqueous solutions.

Methylene blue and methyl orange dye degradation: For the degradation of methylene blue, 0.5 mL of 0.06 M NaBH$_4$ solution was added to 2 mL of 10^{-4} M methylene blue solution in a quartz cuvette. The reaction mixture was stirred vigorously for 5 min to ensure thorough mixing. After this, 200 μL, 300 μL and 200 μL of 10^{-3} M Ag NPs, synthesized from *M. koenigii* (MK), *O. sanctum* (OS) and *M. spicata* (MS), respectively, were added separately to the methylene blue-sodium borohydride (MB-BH) mixture. The reaction was stirred well and the progress of the degradation was monitored by UV-Visible spectroscopy. For the degradation of methyl orange, 20 μL of each OS-Ag NPs, MS-Ag NPs and MK-Ag NPs solution was separately introduced into the reaction mixture. The degradation process was continuously monitored by UV-visible spectroscopy, allowing for the observation of the catalytic activity of Ag NPs in dye reduction.

Catalytic reduction of 4-nitrophenol (4-NP): The reduction was carried out by adding 1 mL of 4-nitrophenol (0.01 M) and 2.5 mL of water to the reaction mixture. Subsequently, 100 μL of 0.5 M NaBH$_4$ was added, followed by the addition of 25 μL of Ag NPs to each mixture. The progress of the reduction was monitored using UV-Visible spectroscopy.

Antibacterial and antifungal studies

Bacterial strains and culture conditions: Gram-negative *Pseudomonas fluorescens* and Gram-positive *Bacillus megaterium* were used in this study and inoculated from -20 ºC storage into 10 mL of nutrient broth and incubated overnight at 37 ºC and 30 ºC, respectively. The bacterial cells (0.1 mL) were centrifuged at 3000 rpm for 3 min, washed once in phosphate buffer saline (PBS) and re-suspended in nutrient broth.

Fungal strains and culture conditions: *Candida albicans* and *Candida parapsilosis* were used in this study and inocu-

lated from -20 ºC storage into 10 mL of nutrient broth and incubated overnight at 30 ºC. The fungal cells (0.1 mL) were centrifuged at 3000 rpm for 1 min, washed in phosphate buffer saline (PBS) [31].

Bacterial inhibition assay: The prepared samples were transferred into 1 mL of bacterial suspension (prepared above) in culture tubes (1.5 mL) and incubated for 24 h. The diluted culture solution from each test was plated on a nutrient agar plate for the bacterial counts. Colony forming units (CFU)/mL on the plate were counted, after incubation overnight.

Fungal inhibition assay: The above procedure for the bacterial inhibition assay was followed for fungal inhibition too.

RESULTS AND DISCUSSION

UV-Vis studies: The colour changed from light yellow to deep reddish-brown, which was visible to the naked eye and the surface plasmon absorption peak, shown in Fig. 1, centered around 435 nm, confirmed the formation of Ag NPs. The plasmon band is broad due to the presence of components from the leaf extract that contribute to the measurement within the spectrophotometric range.
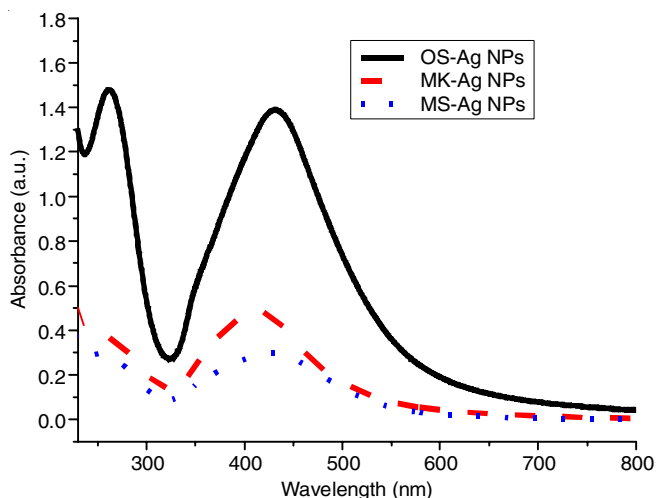
Fig. 1. UV-Vis spectra of green synthesized silver nanoparticles

DLS analysis and zeta potential measurements: Using a Malvern Zetasizer Nano ZS fitted with a 633 nm laser, dynamic light scattering and laser doppler electrophoresis were used to evaluate the nanoparticle size and zeta-potential, respectively. Stable particles are those whose ζ-potential is greater than +30 mV or less than -30 mV. Strong electrostatic repulsion between nanoparticles is indicated by high positive or negative ζ-potential values, which helps in preventing flocculation. According to the particle size distribution graph (Fig. 2), the hydrodynamic diameters of Ag NPs range from 20 to 30 nm. One important determinant of the colloidal Ag NPs long-term stability is their zeta potential. The green-synthesized Ag NPs are significant for having zeta potential values between -13.6 and -22.6 mV.

Morphological studies: The morphology of the synthesized silver nanoparticles revealed that they are spherical in
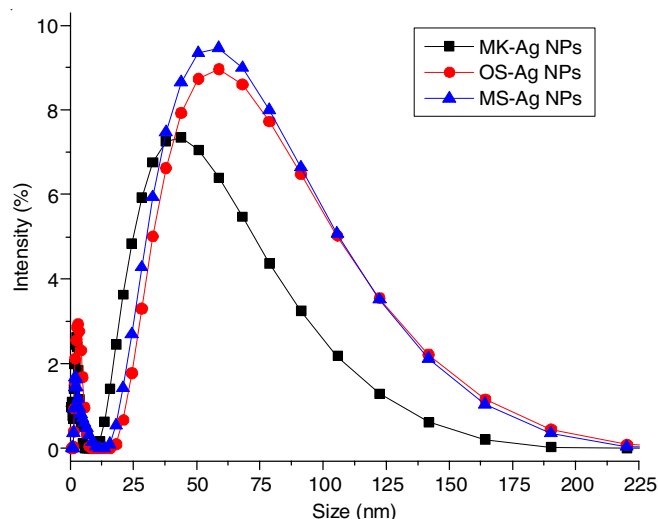
Fig. 2. DLS of green synthesized silver nanoparticles
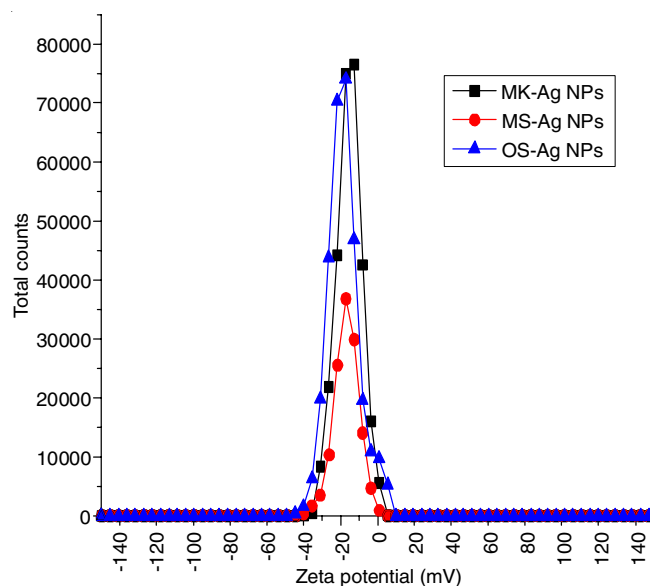
Fig. 3. Zeta potential of OS-Ag NPs, MS-Ag NPs and MK-Ag NPs

shape (Fig. 4) and are uniformly distributed. The phytochemicals present in the extracts may have an impact on the shape and size of nanoparticles. TEM analysis was used to measure the size of the generated silver nanoparticles, which showed a spherical and uniform shape (Fig. 4d). The size of the biosilver nanoparticles ranges from 20 to 30 nm.

Colorimetric sensing of heavy metal: To investigate the metal ions detection ability of green synthesized Ag NPs, 13 metal cations *viz.* K^+, Mn^{2+}, Pb^{2+}, Cu^{2+}, Ni^{2+}, Cd^{2+}, Ca^{2+}, Sr^{2+}, Cr^{2+}, Co^{2+}, Ba^{2+}, Na^+ and Hg^{2+} were analyzed. It was clearly observed that except mercury, no other metal showed any remarkable change in colour and UV-Vis spectra (Fig. 5). Fig. 6 substantiates that only Hg^{2+} shows a colour change from light brown to colourless, which was easily observed with naked eyes.

Catalytic studies: The catalytic degradation activity of green synthesized Ag NPs was evaluated by using methyl orange dye, methylene blue dye and 4-nitrophenol.
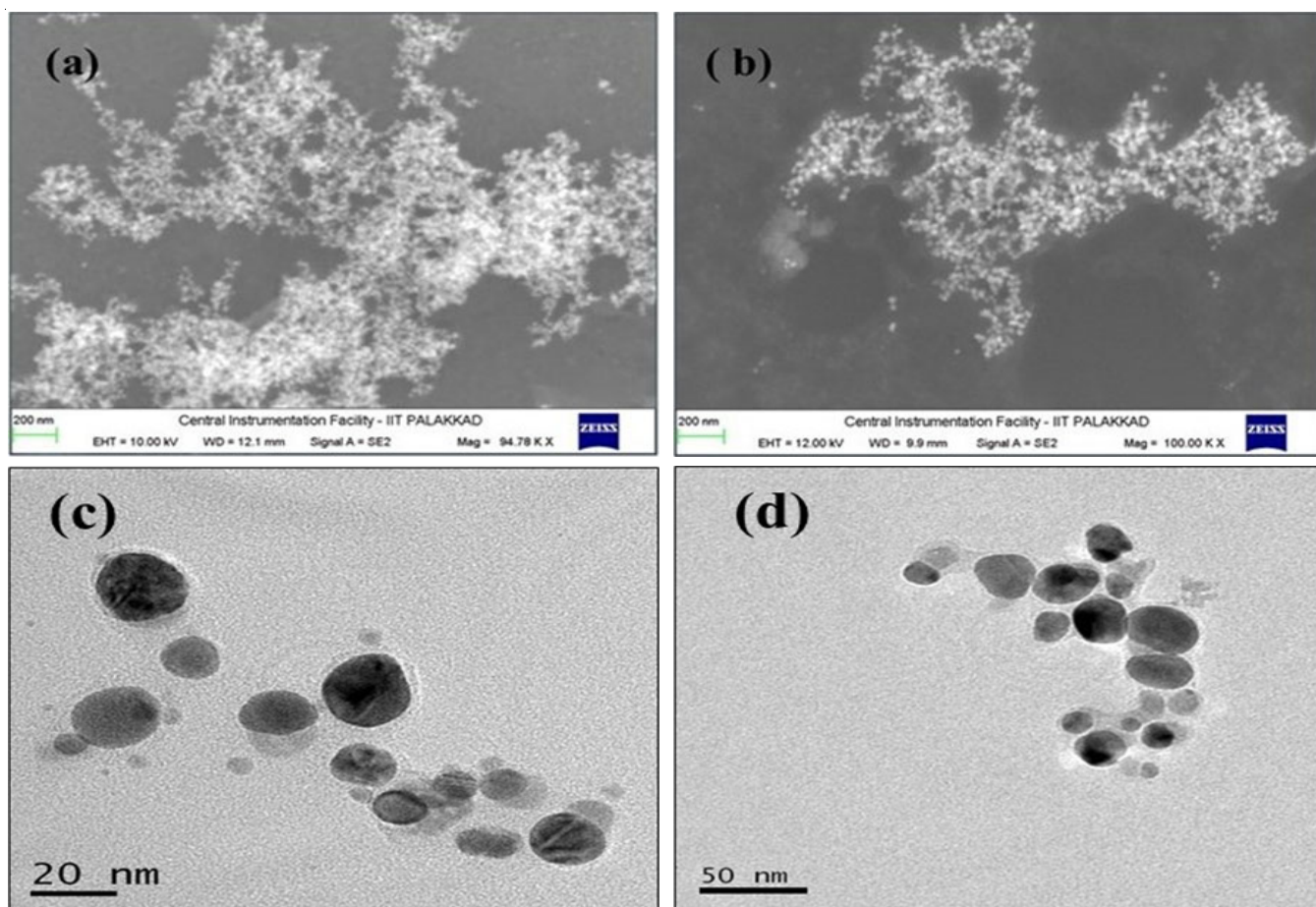
Fig. 4. (a,b) FESEM image of Ag NPs and (c,d) TEM image of Ag NPs
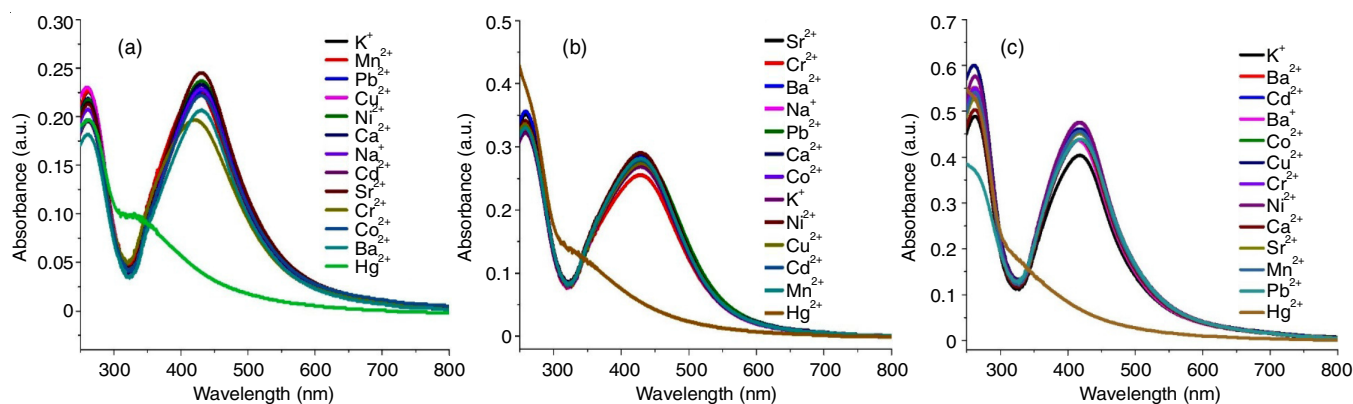
Fig. 5. UV-Vis spectral change during colorimetric sensing of mercury with (a) OS-Ag NPs (b) MS-Ag NPs and (c) MK-Ag NPs
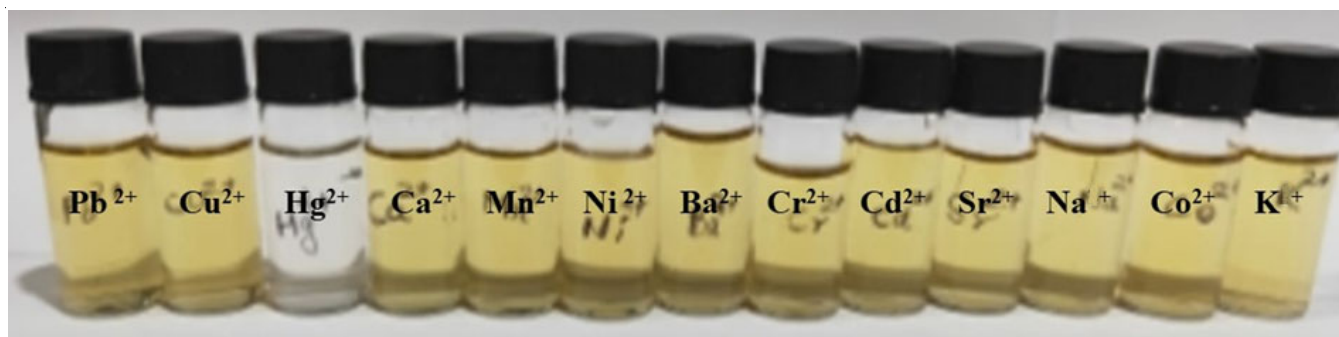
Fig. 6. Photographic images of colorimetric sensing of mercury with MS-Ag NPs

Methylene blue is a heterocyclic aromatic dye exhibiting absorption spectrum at 665 nm, which is due to the $n{\rightarrow}\pi^*$ transition of methylene blue. After the addition of Ag NPs, the peak will decrease within 4-6 min, which indicates Methylene blue was converted into leuco methylene blue (Fig. 7).

Methyl orange dye exhibits characteristic absorption spectrum at 460 nm. After the addition of biogenic Ag NPs to the methyl orange and BH$_4$ reaction mixture, the absorption spectrum at 460 nm gradually disappeared in 4 min and the new peak was formed at 247 nm (Fig. 8). During degradation

reaction, the azo group is reduced to the amino group (Fig. 9) [32].

The catalytic efficiency of Ag NPs for the reduction of 4-nitrophenol to 4-aminophenol using sodium borohydride was also conducted. The characteristic peak of 4-nitrophenol is exhibited at 340 nm, which is shifted to 400 nm by the addition of freshly prepared NaBH$_4$, resulting in the formation of nitrophenolate ions [33]. The absorption intensity of 4-nitrophenolate observed at 400 nm remains unchanged without silver nanocatalyst. From Fig. 10, it was clear that after the
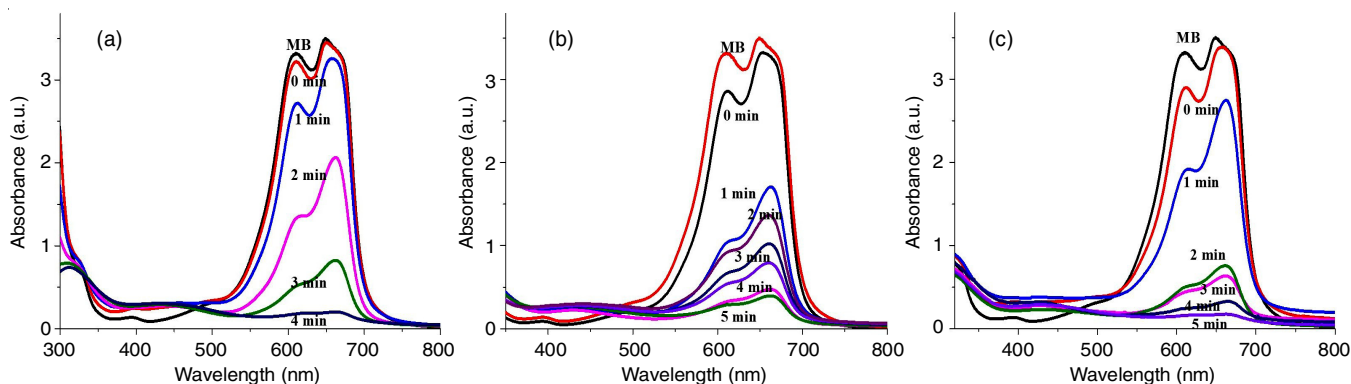
Fig. 7. UV-Vis spectra of methylene blue degradation with (a) MK-Ag NPs, (b) MS-Ag NPs and (c) OS-Ag NPs
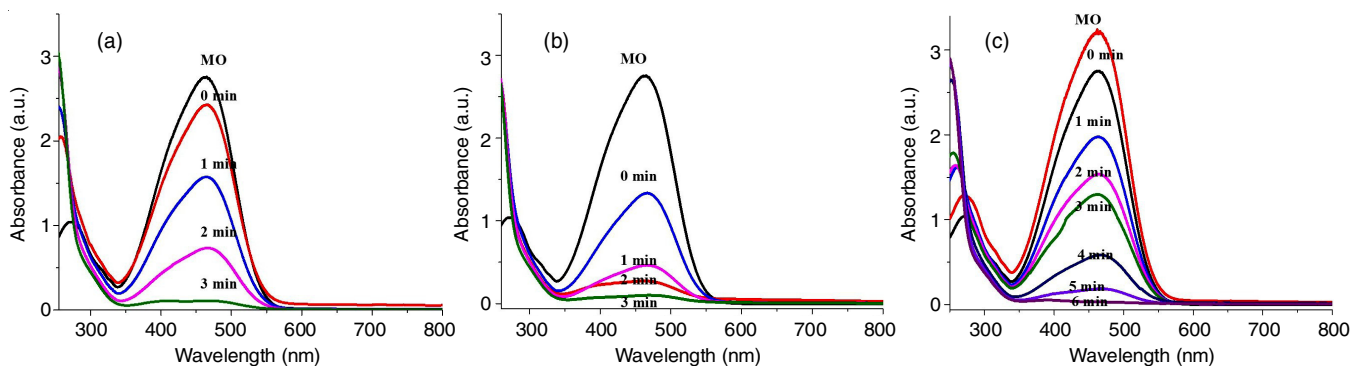
Fig. 8. UV-Vis spectra of methyl orange degradation with (a) MK-Ag NPs, (b) MS-Ag NPs and (c) OS-Ag NPs
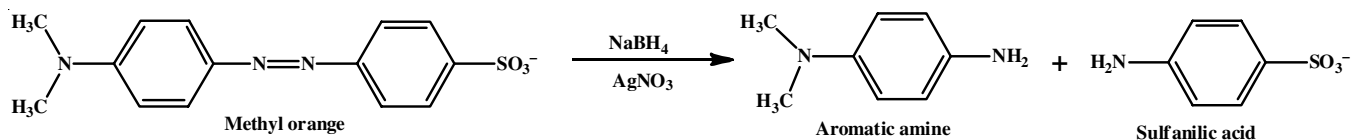
Fig. 9. Schematic representation of methyl orange reduction with silver nanoparticles
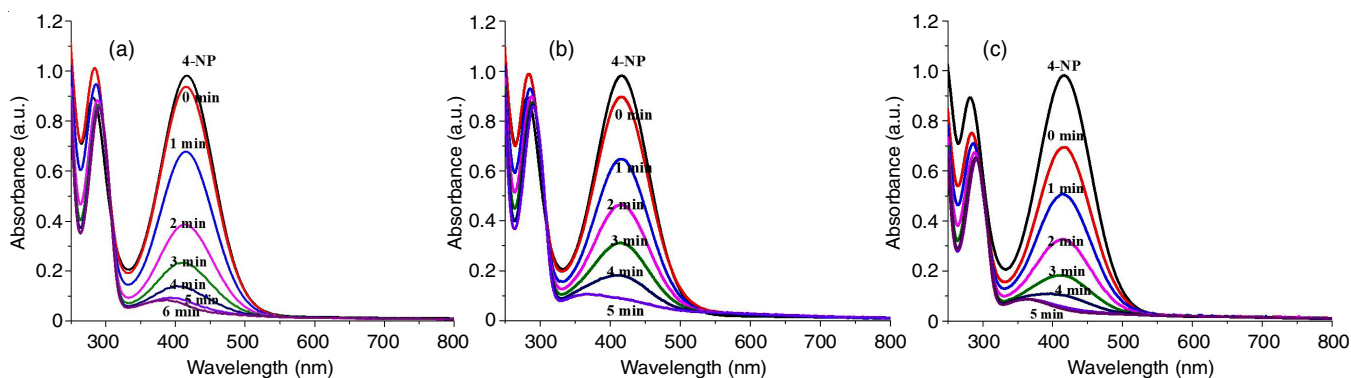
Fig. 10. UV-Vis spectra of 4-nitrophenol reduction with (a) MK-Ag NPs, (b) MS-Ag NPs and (c) OS-Ag NPs

addition of 25 µL of Ag NPs, the peak at 400 nm vanishes and a new peak appears at 280 nm, which corresponds to the formation of 4-aminophenol in 4 min.

Antimicrobial studies

Antibacterial assay: The antibacterial activity of the green synthesized Ag NPs was investigated against the Gram-negative *P. fluorescens* and Gram-positive *B. megaterium* strains. It was observed that control shows considerable colony formation by *P. fluorescens* and *B. megaterium* control (PFC and BMC) after 24 h. However, a significant antimicrobial activity upon addition of Ag NPs were observed. The relative number of colonies of bacterial growth in PBS surrounding Ag NPs is shown in Fig. 11, which indicated that the Ag NPs are active against the bacteria causing sharp declines of bacteria growth. Comparing the inhibition behaviours of bacterial growth for the two strains (*P. fluorescens* and *B. megaterium*), it was found that there were no significant differences in the inhibition extents of both strains.

Antifungal assay: The antifungal activity of the green-synthesized Ag NPs was also investigated against *C. albicans* and *C. parapsilosis.* A significant antifungal activity upon addition of Ag NPs. The relative number of colonies of fungal growth in PBS surrounding Ag NPs is shown in Fig. 12. This indicated

that the Ag NPs are active against the fungus and causing sharp declines of fungal growth. Comparing the inhibition behaviours of fungal growth for the two strains (*C. albicans* and *C. parapsilosis*), it was found that there were no significant differences in the inhibition extents of both strains.

Conclusion

In conclusion, homogenous spherical silver nanoparticles were synthesized by green reduction method using three different leaf extracts of *Murraya koenigi*, *Oscimum sanctum* and *Mentha spicata* as stabilizing and capping agents with 1 mM $AgNO_3$ solution as metallic precursor. The green synthesized Ag NPs of 20-30 nm in size exhibit excellent antibacterial activities against *P. fluorescens* and *B. megaterium* strains. The Ag NPs displayed outstanding antifungal activities against *C. albicans* and *C. parapsilosis* strains. They exhibited selective sensing towards the detection of Hg^{2+} in ppm level in aqueous solutions among the other heavy metal ions studied. The nanoparticles also showed catalytic activity towards the degradation of dyes such as methylene blue, methyl orange and 4-nitrophenol. Present work exhibited an efficient and low-cost biological approach to synthesize the silver nanoparticles with high stability. This green chemistry approach towards the synthesis of silver nanoparticles has many advantages such
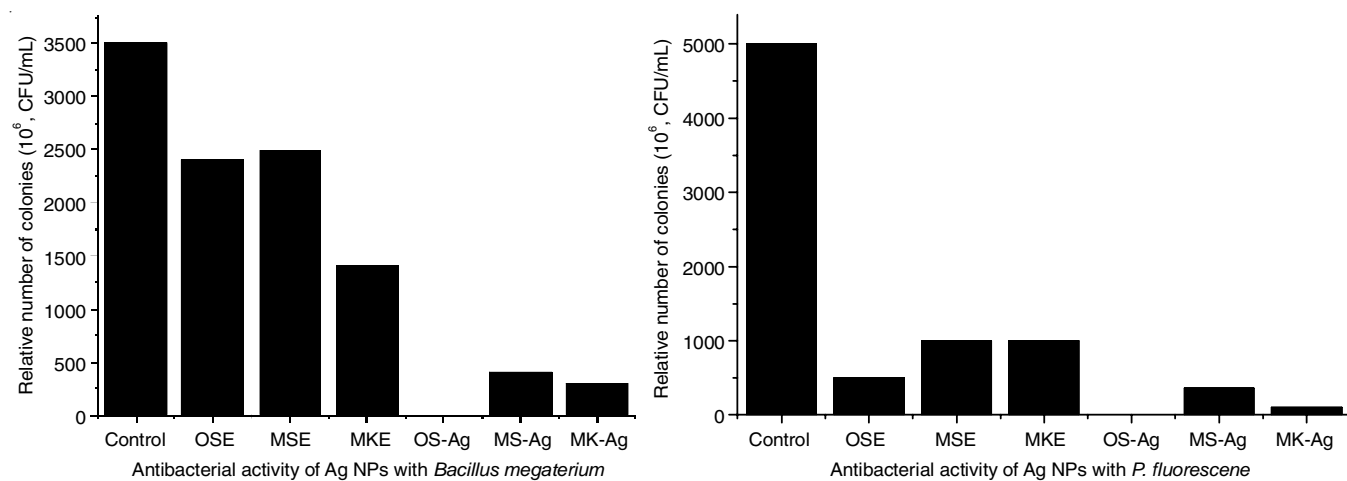
Fig.11. Graphical representation of growth of bacterial colonies *Bacillus megaterium* and *Pseudomonas fluorescens* with silver nanoparticles
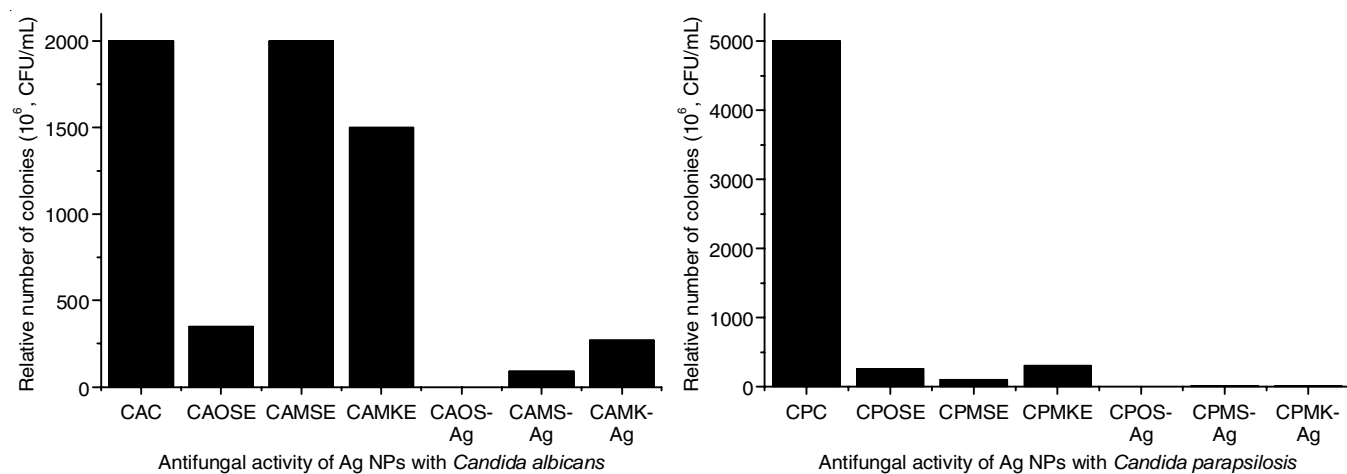
Fig. 12. Graphical representation of growth of fungal colonies *Candida albicans* and *Candida parapsilosis* with silver nanoparticles

as, ease with which the process can be scaled up, economic viability, *etc.*

CONFLICT OF INTEREST

The authors declare that there is no conflict of interests regarding the publication of this article.

REFERENCES

1. S. Iravani, *Green Chem.*, **13**, 2638 (2011);
    https://doi.org/10.1039/c1gc15386b
2. A.S. Aliero, S.H. Hasmoni, A. Haruna, M. Isah, N.A.N.N. Malek and N.A. Zawawi, *Chem. Eng. Commun.*, **212**, 472 (2025);
    https://doi.org/10.1080/00986445.2024.2403117
3. H. Duman, F. Eker, E. Akdasçi, A.M. Witkowska, M. Bechelany and S. Karav, *Nanomaterials*, **14**, 1527 (2024);
    https://doi.org/10.3390/nano14181527
4. P.R. More, S. Pandit, A.D. Filippis, G. Franci, I. Mijakovic and M. Galdiero, *Microorganisms*, **11**, 369 (2023);
    https://doi.org/10.3390/microorganisms11020369
5. M.M. Hossain, A. Hamza, S.A. Polash, M.H. Tushar, M. Takikawa, A.B. Piash, C. Dekiwadia, T. Saha, S. Takeoka and S.R. Sarker, *RSC Pharm.*, **1**, 245 (2024);
    https://doi.org/10.1039/D3PM00077J
6. R. Larayetan, M.O. Ojemaye, O.O. Okoh and A.I. Okoh, *J. Mol. Liq.*, **273**, 615 (2019);
    https://doi.org/10.1016/j.molliq.2018.10.020
7. M.L. Yola, T. Eren, N. Atar and S. Wang, *Chem. Eng. J.*, **242**, 333 (2014);
    https://doi.org/10.1016/j.cej.2013.12.086.
8. Y. Ping, J. Zhang, T. Xing, G. Chen, R. Tao and K.H. Choo, *J. Ind. Eng. Chem.*, **58**, 74 (2018);
    https://doi.org/10.1016/j.jiec.2017.09.009
9. M. Ghaedi, M. Yousefinejad, M. Safarpoor, H.Z. Khafri and M. Purkait, *J. Ind. Eng. Chem.*, **31**, 167 (2015);
    https://doi.org/10.1016/j.jiec.2015.06.020
10. M. Zargar, K. Shameli, G.R. Najafi and F. Farahani, *J. Ind. Eng. Chem.*, **20**, 4169 (2014);
    https://doi.org/10.1016/j.jiec.2014.01.016
11. V. Dhand, L. Soumya, S. Bharadwaj, S. Chakra, D. Bhatt and B. Sreedhar, *Mater. Sci. Eng. C*, **58**, 36 (2016);
    https://doi.org/10.1016/j.msec.2015.08.018
12. V.S. Kumar, B.M. Nagaraja, V. Shashikala, S.S. Madhavendra, B.D. Raju, A.H. Padmasri and K.R. Rao, *J. Mol. Catal. Chem.*, **223**, 313 (2004);
    https://doi.org/10.1016/j.molcata.2003.09.047
13. R. Prucek, J. Tuèek, M. Kilianová, A. Panáèek, L. Kvítek, J. Filip, M. Koláø, K. Tománková and R. Zboøil, *Biomaterials*, **32**, 4704 (2011);
    https://doi.org/10.1016/j.biomaterials.2011.03.039
14. M.T. Reetz and W. Helbig, *J. Am. Chem. Soc.*, **116**, 7401 (1994);
    https://doi.org/10.1021/ja00095a051
15. R. Kaegi, B. Sinnet, S. Zuleeg, H. Hagendorfer, E. Mueller, R. Vonbank, M. Boller and M. Burkhardt, *Environ. Pollut.*, **158**, 2900 (2010);
    https://doi.org/10.1016/j.envpol.2010.06.009
16. C. Marambio-Jones and E.M.V. Hoek, *J. Nanopart. Res.*, **12**, 1531 (2010);
    https://doi.org/10.1007/s11051-010-9900-y
17. M. Venkatesham, D. Ayodhya, A. Madhusudhan, A.S. Kumari, G. Veerabhadram and K.G. Mangatayaru, *J. Cluster Sci.*, **25**, 409 (2014);
    https://doi.org/10.1007/s10876-013-0620-1
18. K. Chaloupka, Y. Malam and A.M. Seifalian, *Trends Biotechnol.*, **28**, 580 (2010);
    https://doi.org/10.1016/j.tibtech.2010.07.006
19. O.V. Salata, *J. Nanobiotechnology*, **2**, 3 (2004);
    https://doi.org/10.1186/1477-3155-2-3
20. R. Tankhiwale and S. Bajpai, *Colloids Surf. B Biointerfaces*, **69**, 164 (2009);
    https://doi.org/10.1016/j.colsurfb.2008.11.004
21. T.V. Duncan, *J. Colloid Interface Sci.*, **363**, 1 (2011);
    https://doi.org/10.1016/j.jcis.2011.07.017
22. B. Ajitha, Y.A.K. Reddy, H.-J. Jeon and C.W. Ahn, *Adv. Powder Technol.*, **29**, 86 (2018);
    https://doi.org/10.1016/j.apt.2017.10.015
23. Y.Y. Ho, D.S. Sun and H.H. Chang, *Int. J. Mol. Sci.*, **21**, 7082 (2020);
    https://doi.org/10.3390/ijms21197082
24. A. Kumar, S.R. Shah, T.J. Jayeoye, A. Kumar, A. Parihar, B. Prajapati, S. Singh and D.U. Kapoor, *Front. Nanotechnol.*, **5**, 1175149 (2023);
    https://doi.org/10.3389/fnano.2023.1175149
25. A.K. Ilunga and R. Meijboom, *J. Mol. Catal. Chem.*, **411**, 48 (2016);
    https://doi.org/10.1016/j.molcata.2015.10.009
26. J. Saha, A. Begum, A. Mukherjee and S. Kumar, *Sustain. Environ. Res.*, **27**, 245 (2017);
    https://doi.org/10.1016/j.serj.2017.04.003
27. M. Nasrollahzadeh, M. Atarod, B. Jaleh and M. Gandomirouzbahani, *Ceram. Int.*, **42**, 8587 (2016);
    https://doi.org/10.1016/j.ceramint.2016.02.088
28. S.S. Dash, B.G. Bag and P. Hota, *Appl. Nanosci.*, **5**, 343 (2015);
    https://doi.org/10.1007/s13204-014-0323-4
29. M. Nasrollahzadeh, S.M. Sajadi and M. Maham, *J. Mol. Catal. Chem.*, **396**, 297 (2015);
    https://doi.org/10.1016/j.molcata.2014.10.019
30. K. Muthu and S. Priya, *Spectrochim. Acta A Mol. Biomol. Spectrosc.*, **179**, 66 (2017);
    https://doi.org/10.1016/j.saa.2017.02.024
31. R. Mourad, F. Helaly, O. Darwesh and S.E. Sawy, *Cont. Lens Anterior Eye*, **42**, 325 (2019);
    https://doi.org/10.1016/j.clae.2019.02.007
32. R. Vijayan, S. Joseph and B. Mathew, *Particul. Sci. Technol.*, **37**, 809 (2019);
    https://doi.org/10.1080/02726351.2018.1450312
33. T.L. Pham, V.D. Doan, Q.L. Dang, T.A. Nguyen, T.L.H. Nguyen, T.D.T. Tran, T.P.L. Nguyen, T.K.A. Vo, T.H. Nguyen and D.L. Tran, *RSC Adv.*, **13**, 20994 (2023);
    https://doi.org/10.1039/D3RA02754F